

The Causes and Effects of Adverse Space Weather

Jih-Kwin Chao^{1, *} and Lou-Chuang Lee^{2, 3}

(Manuscript received 3 February 2000, in final form 1 March 2000)

ABSTRACT

Space weather refers to highly disturbed conditions on the sun, in the solar wind, magnetosphere, ionosphere, and thermosphere that can influence the performance and reliability of space-borne and ground-based technological systems and can endanger human life and health. Adverse changes in the near-Earth space environment can cause disruption of satellite operations, communications, navigation, and electric power distribution grids, leading to a variety of socioeconomic losses. This paper discusses some of the causes that lead to adverse space environment. The sources are believed to be on the sun. The propagation of these sources through the interplanetary space is reviewed. Finally, the interactions of the interplanetary disturbances with the earth's magnetosphere that include bow shock, magnetopause, magnetosphere, and ionosphere are considered. The example of the June 24-28, 1999 event is given to demonstrate the solar/interplanetary/magnetosphere inter-relationships. There is no doubt that the future COSMIC project will be important for the study of adverse space weather.

(Key words: Adverse space weather, Space weather, Solar-terrestrial physics)

1. INTRODUCTION

In order to minimize the damage to technological systems that can result from severe geomagnetic disturbances, much attention has been paid to the prediction of storms and substorms (Joselyn, 1995). It is hoped that the solar eruptions can provide a key predictor, and the subsequent propagation of the solar generated disturbances to 1 AU that produce severe geomagnetic disturbances can be determined. At present the best understanding of the relationships between solar eruptions and resulting geoeffective solar wind events is statistical (e.g., Joselyn and McIntosh, 1981; Wilson and Hildner, 1984, 1986; Gosling et al, 1991; Gosling, 1993). For given solar wind parameters, such as the solar wind speed V , number density N , IMF B and possibly other parameters, the geomagnetic storms are modeled by estimation

¹Institute of Space Science, National Central University, Chung-Li, Taiwan, ROC

²Physics Department, National Cheng Kung University, Tainan, Taiwan, ROC

³National Space Program Office, Hsin-Chu, Taiwan, ROC

* *Corresponding author address:* Dr. Jih-Kwin Chao, Institute of Space Science, National Central University, Chung-Li, Taiwan, ROC; E-mail: jkchao@jupiter.ss.ncu.edu.tw

of the geoeffective parameters Dst and AE (e.g., Burton et al., 1975 ; Perreault and Akasofu, 1978 ; Akasofu and Chao, 1980 ; Sharma et al., 1993 ; Vassiliadis et al., 1995; Wu and Lundstedt, 1996 ; Chen et al, 1997).

On the other hand, the study of the solar source of geomagnetic storms has been continued for a long period (Dryer, 1982 ; 1994; Gosling et al., 1991; Zhao and Hoeksema, 1995 ; Hundhausen, 1993). The relation between solar flares and strong magnetic storms has long been recognized. Transient interplanetary (IP) shock waves have been associated with flares (Chao and Lepping, 1974; Hundhausen, 1972). However, many IP shocks are found no association with flares. Chao (1974) noted that the associations of IP shocks with their flare origin are not totally satisfactory. The association of a shock wave at 1 AU with a particular flare is not always possible. Some shocks can be associated with large flares while some others can be attributed only to small ones. On the other hand, some large flares do not produce IP shocks near the earth. Later, Tang et al. (1989) showed that there is no correlation between the flare parameters and the strength of the IP shock at Earth. The sudden eruption of solar prominences has also been invoked as a source of geomagnetic perturbations (Joselyn and McIntosh, 1981; Wright and McNamara, 1983). Their associations are not good (Bravo et al, 1999).

Coronal mass ejections (CMEs) were first observed in the 1970's as changes in coronal structure that occur on a time scale from a few minutes to several hours (Gosling, 1975 ; Dryer, 1982; Hundhausen, 1993). Observations of CMEs on the Solwind coronagraph on board the P78-1 satellite have been compared with transient interplanetary shocks observed by the Helios 1 spacecraft from 1979 to 1983 by Sheeley et al. (1985). Virtually every shock observed by Helios was preceded by a CME observed by Solwind. Since then, it has been widely accepted that CMEs are the pistons, which drive IP shocks ahead. When entering IP space, CMEs are often called interplanetary magnetic cloud (IMC). A high-density region between the preceding shock and the boundary of the IMC resembles the magnetosheath of the terrestrial magnetosphere (Bravo et. al., 1999). Hence IMCs can be called as an interplanetary magnetosphere. IMCs contain coronal materials, which are much less dissipative than blast waves, and thus can propagate to a large distance in IP space. It is these IMCs, which often carry large southward IMF, and enhanced momentum flux due to compression by the preceded shock, that can generate adverse space weather (Gonzalez and Tsurutani, 1987).

During the IMC passage, the earth's bow shock and magnetopause will be compressed substantially. Often the magnetopause is pushed to the geosynchronous orbit (Shue et al., 1998). The positions of the bow shock can also fluctuate in large amplitude at short time intervals (Wu et. al. 2000, to be published). Under such interactions between the IMCs and the Earth's magnetosphere, energetic solar and magnetospheric charge particles (Baker et al., 1990), geomagnetic storms and magnetospheric substorms are also initiated. Adverse space weather is related to their occurrence. Within the magnetosphere, high-latitude convection pattern and the related electrodynamic parameters are changed under a direct result of solar wind/magnetosphere/ionosphere interactions (Richmond et al., 1998). Field-aligned currents and Alfvén waves are also generated (Ma and Lee, 1999). It is anticipated that the whole ionosphere including the equatorial anomaly regions will be under the influence of adverse space weather.

In this paper, we will give the example of the June 24-29, 1999 event to demonstrate a series of interactions starting from solar surface and ending on the ground. On the solar side,

we use the data from SOHO's EIT and LASCO coronagraph data to identify the solar event. The source surface magnetic field data are obtained from Wilcox Observatory of Stanford University (Zhao and Hoeksema, 1995). A kinematic code (Hakamada and Akasofu, 1982) is used to calculate the propagation from the source surface to 1 AU. Interplanetary magnetic field and plasma data of WIND and Geotail are used as the upstream input parameters for predictions of the positions and shapes of the earth's bow shock and magnetopause. The IZMEM model (Papitashvili et al., 1999) is used to calculate the field-aligned currents in the polar region. Future calculations will use a more sophisticated AMIE code (Richmond and Kamide, 1988) for this purpose.

It is believed that the scheme we demonstrate is a useful one not only for understanding the physics of the couplings between different regions of the solar-terrestrial environment but also possibly for space weather prediction.

2. THE SOLAR SOURCE

The relation between solar flares, transient IP shocks and strong geomagnetic storms has long been recognized (Dryer, 1984). Therefore, solar flares were considered as the most likely solar cause for geomagnetic storms. However, more recent observations on board satellites from coronal and near-surface solar event measurements suggest that the source of the storms is coronal mass ejections (Sheeley et al; Harrison, 1994; Webb and Hundhausen, 1987). Recently Brave et al (1999) found the percentage of solar associations of interplanetary magnetic clouds (IMCs) are 51% for H_{α} flare, 21% for filament eruption, 7% for both of the previous two and 15% for neither of them. From all those studies, it is practically reasonable to assume the solar source is the CMEs for space weather studies. In order to identify a solar source and use it for prediction purpose, we use a kinematic code. This code was designed by Hakamada and Akasofu (1982) and modified by Akasofu and Fry (1986) and Sun et al. (1985). This method combines the magnetic field frozen-in property and some observational property of the solar wind to construct a 3-D solar wind model. It is useful for the study of large structures in the solar wind particularly the large disturbances generated by IMCs. There are three important assumptions made in the model:

1. The background solar wind speed variations are assumed to change with the solar magnetic latitude λ as follows.

$$V(\text{km/s})=700(1-1/\cosh(0.06|\lambda|))+300 \quad \text{for } 0 < |\lambda| \leq 30^{\circ}$$

$$V(\text{km/s})=775 \quad \text{for } 30^{\circ} < |\lambda|$$
2. The solar dipole axis makes an angle χ with the solar rotational axis and varies slowly with the sunspot variations.
3. At $2.5 R_{\odot}$ (solar radii) from the sun, it is assumed that the solar wind flows with the frozen-in magnetic field.
4. The source surface magnetic field at $2.5 R_{\odot}$ is routinely calculated from the Wilcox Solar Observatory of Stanford University. Therefore, the solar wind variations on the source surface are following the variations of the magnetic field. Solar disturbances caused by a

CME or a filament eruption event (FD) are assumed to be spherical symmetric to the radial direction on the source surface and their intensities decrease from the center of the source following a Gaussian distribution

The CMEs are from the coronagraph data of SOHO and FDs obtained from the Geophysical data published by World Data Center A. With the information of the initial disturbance and the ambient solar wind, simulation starts from the source surface at $2.5 R_{\odot}$ from the Sun.

3. INTERPLANETARY SOURCE

Because of the rotation of the Sun, the solar wind and the disturbance entering the interplanetary space will interact with the ambient solar wind originating from different longitudes on the solar surface. This interaction can create additional source for geomagnetic storms. Since the direct cause for storms is a large southward IMF B_z , we look for processes that can generate such a component.

A CME in general is composed of a bright loop, a dark region and a filament or prominence close to the Sun (Hundhausen, 1993, Tsurutani and Gonzalez, 1997; Tsurutani et al., 1999). When entering IP space, the material of the CME is called a driven gas (Bame et al., 1979; Hirshberg et al, 1970). Occasionally, magnetic fields of the given gas have the form of a magnetic cloud or giant flux rope (Burlaga et al, 1987; Klein and Burlaga, 1982). This flux rope will have a B_z component. When the material carrying the magnetic cloud has a speed greater than the ambient solar wind by more than the ambient fast wave speed, fast shock wave will form. This MHD fast shock can compress the upstream magnetic field substantially. If a moderate southward B_z already exists upstream, a large southward B_z will be generated. When it reaches the magnetosphere, a large storm will be initiated. Fast MHD shock can generate the storm efficiently.

Interplanetary shock waves can be grouped into two types. The first type consists of corotating shocks, which are generated by interactions of solar wind streams. The lifetime of these streams may be longer or shorter than one solar rotation period. Hence, the corotating shocks do not necessarily have a recurrence tendency of 27 days (a solar rotational period). The second type consists of transient shocks generated by IMCs. Non-linear large amplitude waves can steepen into fast shocks (Chao, 1973). Both these two types of shocks can amplify the ambient southward B_z to produce the interplanetary cause for geomagnetic storms. Numerical and empirical models have been proposed for this generation mechanism.

The compressed region between the driver gas and the shock wave can be called the sheath region, which is generated in interplanetary space. In principle, the strength and the direction of this B_z can be predicted when the undisturbed source surface magnetic fields and solar wind speeds are known (Wu and Dryer, 1996). Large amplitude Alfvén waves and turbulence when compressed by the shocks may also be the source for storms when large B_z 's are present. Tsurutani and Gonzalez (1997) have listed six types of possibilities of how large southward B_z are created: (1) shocked southward fields (Tsurutani et al., 1988), (2) bending of the heliospheric current sheets (HCS) (Tsurutani et al., 1984), (3) amplification of Alfvén waves and turbulence (Tsurutani et al., 1995), (4) draped magnetic fields in the sheath region (Midgley and Davis, 1963 ; Zwan and Wolf, 1976; McComas et al., 1989), (5) equinoctial B_y

effect (Russell and McPherron, 1973) and (6) fast stream-HCS interactions (Odstroil and Pizzo, 1999). It is hoped that kinematic simulation can account for some of the above listed possibilities.

4. MAGNETOSPHERIC EFFECTS

The supersonic solar wind impinges on the Earth's magnetosphere generating the magnetopause (MP) and bow shock (BS). Both MP and BS are never been found to disappear. During the recently observations by the ISTP satellites WIND, ACE, Geotail and IMP-8 on May 11, 1999, the number density of solar wind had dropped to below 1 per cubic cm for more than half a day. Both BS and MP have been found to cross some of these satellites at large distances from the Earth. On the other hand, under some extreme solar wind conditions when the high solar wind speed, number density and large southward B_z prevail, the MP and BS can be pushed much closer to the Earth. Sometimes the MP moves inside the geosynchronous orbit and some orbiting satellites may enter the magnetosheath and be exposed to the solar wind and fields. Some vulnerable satellites will have difficulties in coping with highly variable fluctuations of the fields and energetic solar wind particles. Thus, forecasts of those geosynchronous MP crossings are very important to the safety of geosynchronous satellites.

The locations of the MP are not only important for modeling the magnetosphere but also essential in space weather forecasts. Models for the size and shape of the MP are plenty (Fairfield, 1971; Formisano et al., 1979; Petrinec and Russell, 1993, 1996; Roelof and Sibeck, 1993; Shue et al., 1997, 1998). Only a few of them can be used for predictions. Shue et al. (2000) first compare two models (Petrinec and Russell, 1996; Shue et al., 1998) to test the capability of predictions of geosynchronous MP crossings by GOESs satellite using seven years of data. Yang et al. (2000) improve the prediction of Shue et al. (2000) by using a new model derived from a carefully selected database of MP crossings.

The models for the Earth's BS are also important for space weather studies (e.g., Fairfield, 1971; Formisano, 1979; Slavin and Holzer, 1981; Farris and Russell, 1994; Cairns et al., 1995; Cairns and Lyon, 1995; Peredo et al., 1995; Bennett et al., 1997; Wu et al., 2000). Recently, Chao et al. (2000) have selected a database of BS crossings from Geotail using only the multiple crossing events with quiet upstream conditions. The satellite WIND is used as a monitor to obtain the upstream parameters D_p , B_z , β and M_{ms} , which are the solar wind dynamic pressure, IMF B_z , plasma beta and magnetosonic Mach number respectively. A model for the size and shape of the BS is thus derived. This model is able to predict the IMC induced BS crossings very accurately. As an example, the 26 Geotail's BS crossings, which are induced by the October 18-20, 1995 IMC event, are correctly predicted by this model except one. Solar wind disturbance induced BS and MP crossings for a selected event will be demonstrated in the next section.

Large disturbances within an IMC may have a large solar wind-magnetosphere energy coupling function ε (Perreault and Akasofu, 1978; Akasofu, 1981; Kan and Lee, 1979). The coupling function is given by Perreault and Akasofu (1978) as follows:

$$\varepsilon = VB^2 \sin^4(\theta/2)L_0^2$$

where V =the solar wind speed, B the IMF, $L_0 = 7 R_e$,

and $\theta = \tan^{-1}(|B_y/B_z|)$ for $B_z > 0$; $\theta = 180^\circ - \tan^{-1}(|B_y/B_z|)$ for $B_z < 0$.

In Fig. 1, an example is given for the February 10, 1969 event. It can be seen that the storm sudden commencement (ssc) starts at 20:21 UT and is followed immediately by intense substorm activity as indicated by the AE index. The IMF B_z component was positive for a few

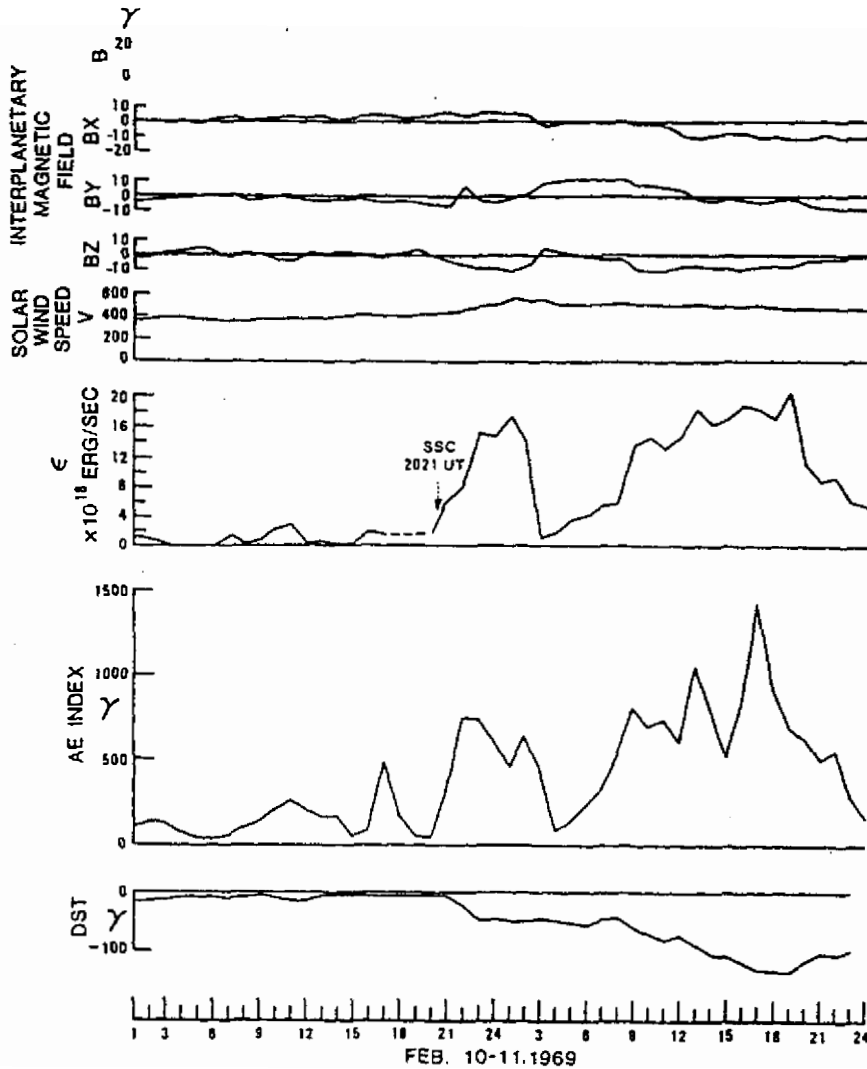


Fig.1. The interplanetary magnetic field (IMF) B , the three components (B_x , B_y , B_z), the solar wind speed V , the solar wind - magnetosphere coupling function ϵ , the magnetosphere substorm index AE and the ring current intensity index Dst for the February 10-11, 1969 storm (Akasofu and Chao, 1980)

hours prior to the S.S.C. The geomagnetic storm starts after the S.S.C. as indicated by the Dst changes. The reasonably good correlation between the AE and the coupling function is apparently noticed. This coupling function can be a good indicator for space weather prediction.

It has been demonstrated in many studies that the large-scale ionospheric convection at high latitudes is primarily controlled by IMF B and solar wind dynamic pressure outside the magnetosphere. The couplings of solar-wind/ magnetosphere/ ionosphere determine the patterns of high-latitude convection and related electrodynamic parameters in the ionosphere. Models of inner magnetospheric convection require knowledge of the electric potential distribution around the polar cap boundary. Similarly, models of thermospheric dynamics need to know the plasma convection at high latitudes in order to model correctly the effects of ion drag and Joule heating. A model is designed for this kind of study, called AMIE (The Assimilative Mapping of Ionospheric Electrodynamics), which is used to synthesize collections of diverse data relating to high-latitude ionospheric electrodynamics into coherent patterns of conductivities, electric fields and currents, and related parameters (Richmond, 1992; Richmond et al., 1998). At present, AMIE is a specification model rather than a forecast model, although its mathematical structure could allow inclusion of time as an additional dimension, which would permit temporal extrapolation. Nonetheless, this specification model can be used to help initialize forecast models of thermospheric winds and composition, ionospheric electron density, and inner-magnetospheric particle populations. Another recent model designed for the study of ionospheric convection patterns is the IZMEM model (The IZMIRAN Electrodynamic Model). Both models can deduce the field-aligned current system in the polar cap. For a satellite at a typical altitude of 800 km the toroidal component of ionospheric current produces a relatively weak magnetic perturbation. By contrast, the field-aligned current system can produce relatively strong magnetic perturbations at satellite altitudes (Richmond and Kamide, 1988). A field-aligned current system calculated from the IZMEM model for the period June 24-29 is given in the next section. An origin of the field-aligned currents has been proposed by (Ma and Lee, 1999). They have carried out a three-dimensional compressible MHD simulation to study the generation of field-aligned currents and Alfvén waves by magnetic reconnection. The results indicate that the presence of IMF By leads to a shift of the reversal site between the downward and upward field-aligned currents that may contribute to the observed region 1 field-aligned currents near noon in the polar ionosphere. This result can be incorporated into the AMIE model to study solar-wind/ magnetosphere coupling.

5. THE JUNE 24-29, 1999 EVENT

In this section, we present observations and analyses of a solar disturbance and the associated IP disturbances that lasted for a little over two days and were observed at 1 AU by ISTP satellites. Such disturbances interact with Earth's bow shock and magnetopause causing their positions and shape to change. The interactions may also influence the polar as well as the equatorial ionosphere. The IPEI payload on ROCSAT-1 observes "bubbles" in the equatorial region of the ionosphere during the passage of this disturbance.

(1) Identification of solar source

A review of possible solar activities, which can be related to the interplanetary disturbance observed at 1 AU from 0200 UT of June 26 to 0300 UT of June 28, shows that two flares and one filament eruption (DSF) occurred at 1818 (N22E37), June 22, 0649(N23E42), June 23, and 1051 UT (N33E09), June 24, respectively, are the possible sources for the event. The observations provided by the LASCO and EIT on board SOHO also reveal solar disturbances at 1400 UT, June 24. Figure 2 shows the observations of the coronal disturbance and the flare activity by LASCO and EIT respectively. LASCO and EIT show a CME and a region of flare activity, respectively, at this time. This solar disturbance will be assumed as our solar source for this event.

(2) Interplanetary propagation

These disturbances and solar wind will start from the source surface. The source surface of the magnetic field measurement is obtained from Wilcox Observatory of Stanford University. One Carrington Rotation (no. 1951) of the Solar Magnetic Field Synoptic Chart is shown in Fig. 3 where the projections of the locations of the Earth and the origin of the disturbances are indicated by a "*" and "O" respectively. With this information, the kinematic code is used to calculate the propagation of disturbances in 3-dimension interplanetary space. Solar wind is assumed to have a radial propagation from the source surface at $2.5 R_{\odot}$ from the Sun. The magnitude of the solar wind speed is assumed to be proportional to the magnetic field strength. With the frozen-in condition assumed, the magnetic fields are carried to IP space. Without any disturbance on the source surface, the magnetic fields are assumed to be in the radial directions. When there is a disturbance added on the source surface with intensities of the velocities decreasing from the center of the source following a Gaussian distribution, the magnetic field will be stretched such that a non-radial component will be generated. This will be the source for B_z component. Figure 4 is a plot of the projected magnetic field line of force on the solar equatorial plane. Outward field is indicated by dash curves and inward field by solid curves. Compression and rarefaction of field lines can be easily noticed from the curves. The simulation starts on 1818 UT, June 22 when the first disturbance is initiated. The circle is the position of the Earth. The first plot shows the IP magnetic fields projected on the ecliptic plane at 0000 UT, June 24. The second one is for 0000 UT, June 25 when all the disturbances have already left the Sun. One can find that the first disturbance reaches 1 AU in late June 25. The kinematic code maps the source surface magnetic field structures in interplanetary space where the sectors of inward and outward magnetic fields are clearly seen. Fast and slow streams originating from different polarities of the solar surface can form the sector structures and interaction regions. Therefore, this code is also good for prediction of the arrival of corotation shocks due to fast- and slow- stream interactions. We would like to point out the discontinuity of field lines at longitude 0° or 360° . It is not real because the source surface given in Fig. 3 we use is not taken simultaneously. Since we are interested in the region far from this longitude, our results are not affected by this discontinuity. The simulated disturbance as seen at the Earth's position is shown in Fig. 5 where the solar wind radial velocity V , number density N , IMF B and its latitude Θ and longitude Φ are respectively shown from top to bottom. The disturbance arrives at the Earth in late June 25 and is so strongly compressed in its frontal part that a shock is formed at the leading edge. The whole event lasts until in early June 28. Small northward and then a little southward IMF B_z is observed inside the compressed sheath region

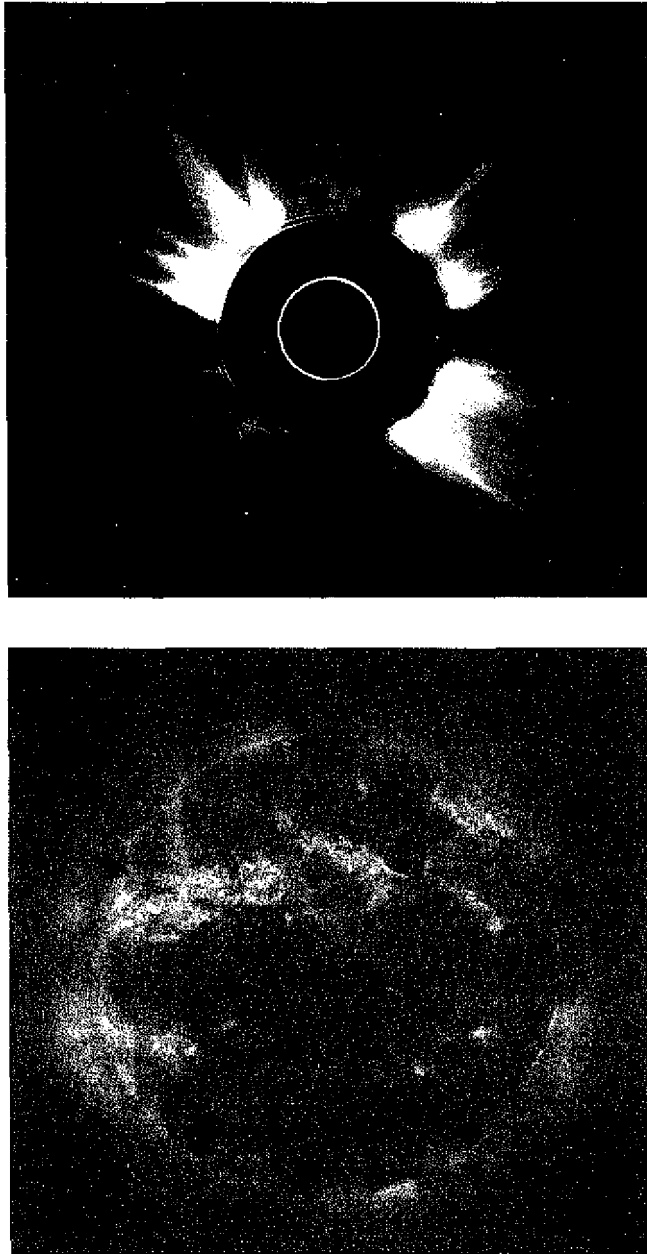


Fig. 2. The EUV Imaging Telescope (EIT) (top) and the Large Angle Spectroscopic Coronagraph (LASCO) (bottom) observations of solar activities occurred near 1400 UT June 24, 1999. The EIT shows an active region on the north-east part of the disk and LASCO shows a CME on the north-east limb. A filament eruption is also observed during the period 1051-1418 UT, June 24, 1999 at N33E09.

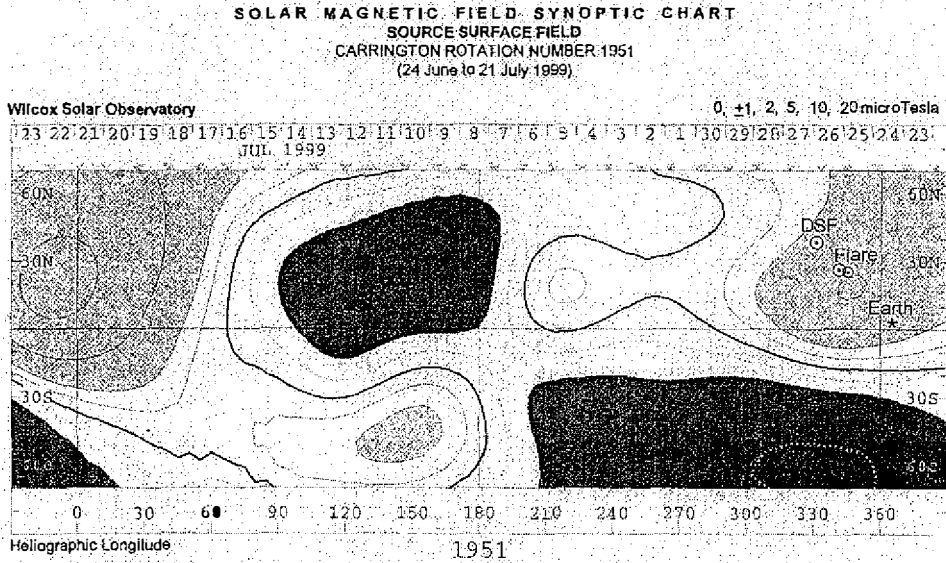


Fig. 3. A solar magnetic field synoptic chart of the source surface field for Carrington rotation number 1951 (June 24 to July 21, 1999). The positions of the Earth and the three possible solar sources for the June 24-28, 1999 event are projected on the source surface located at $2.5 R_{\odot}$ from the Sun. The solid curve maps the positions of the neutral sheet in interplanetary space.

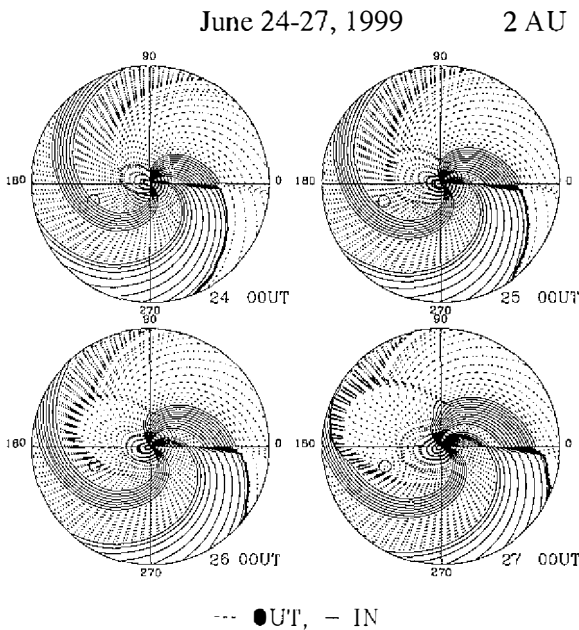


Fig. 4. The ecliptic plane plots of the disturbed IMF for the June 24-27, 1999 event. The top-left one is for 0000 UT, June 24 and the top-right for 0000 UT, June 25. The last one at bottom-right is for 0000 UT, June 27. Three interplanetary disturbances and co-rotation streams are interacting with one another.

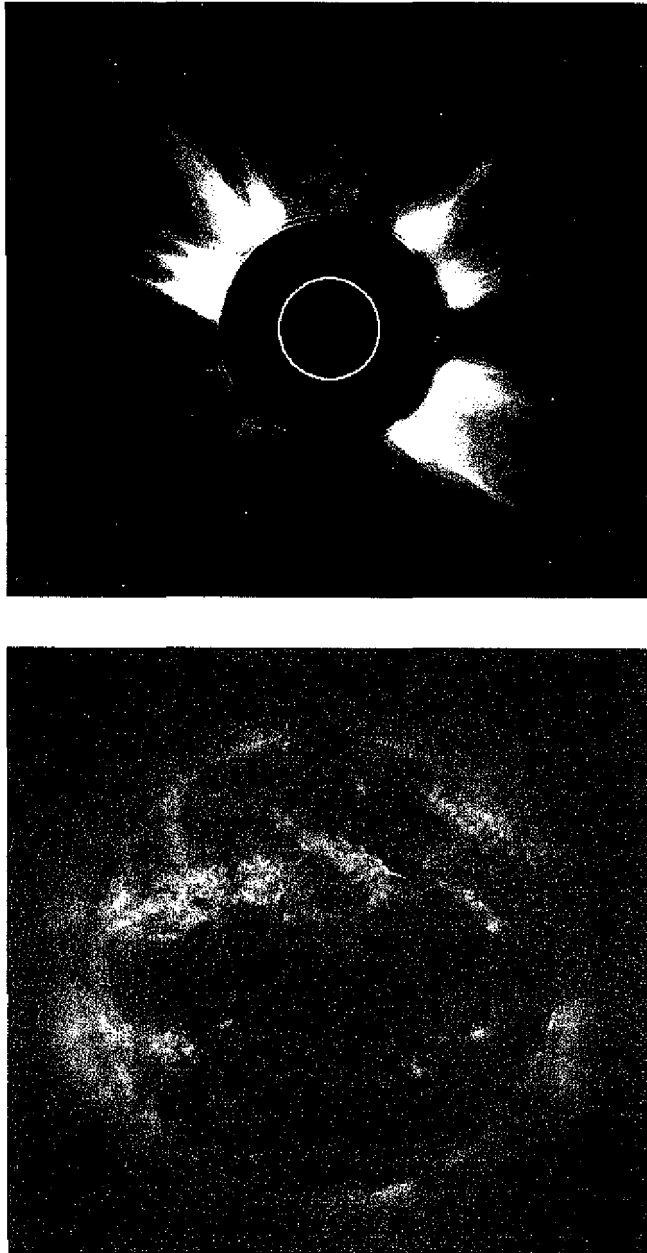


Fig. 2. The EUV Imaging Telescope (EIT) (top) and the Large Angle Spectroscopic Coronagraph (LASCO) (bottom) observations of solar activities occurred near 1400 UT June 24, 1999. The EIT shows an active region on the north-east part of the disk and LASCO shows a CME on the north-east limb. A filament eruption is also observed during the period 1051-1418 UT, June 24, 1999 at N33E09.

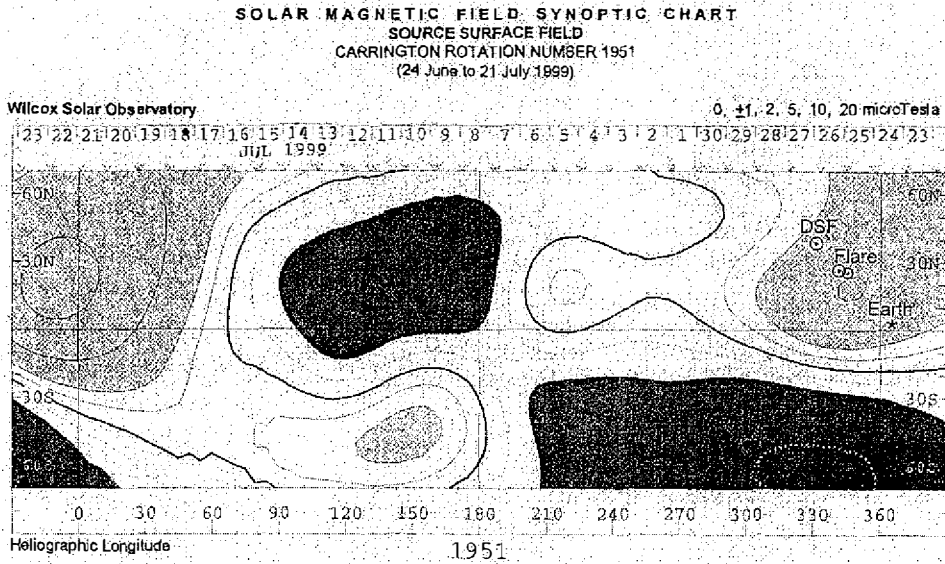


Fig. 3. A solar magnetic field synoptic chart of the source surface field for Carrington rotation number 1951 (June 24 to July 21, 1999). The positions of the Earth and the three possible solar sources for the June 24-28, 1999 event are projected on the source surface located at $2.5 R_{\odot}$ from the Sun. The solid curve maps the positions of the neutral sheet in interplanetary space.

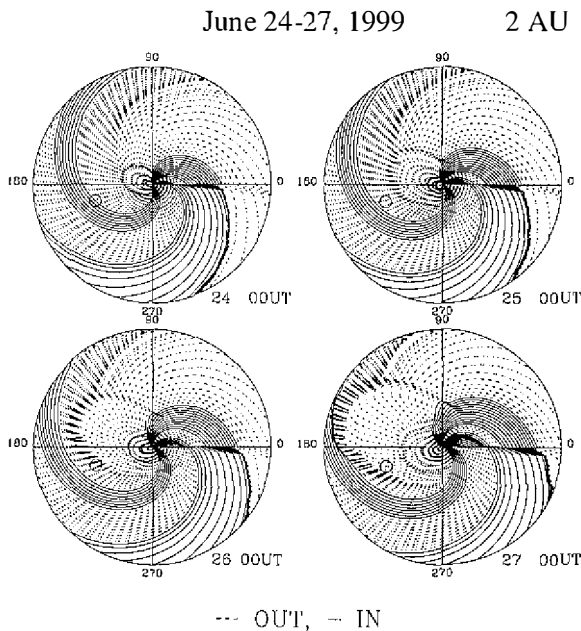


Fig. 4. The ecliptic plane plots of the disturbed IMF for the June 24-27, 1999 event. The top-left one is for 0000 UT, June 24 and the top-right for 0000 UT, June 25. The last one at bottom-right is for 0000 UT, June 27. Three interplanetary disturbances and co-rotation streams are interacting with one another.

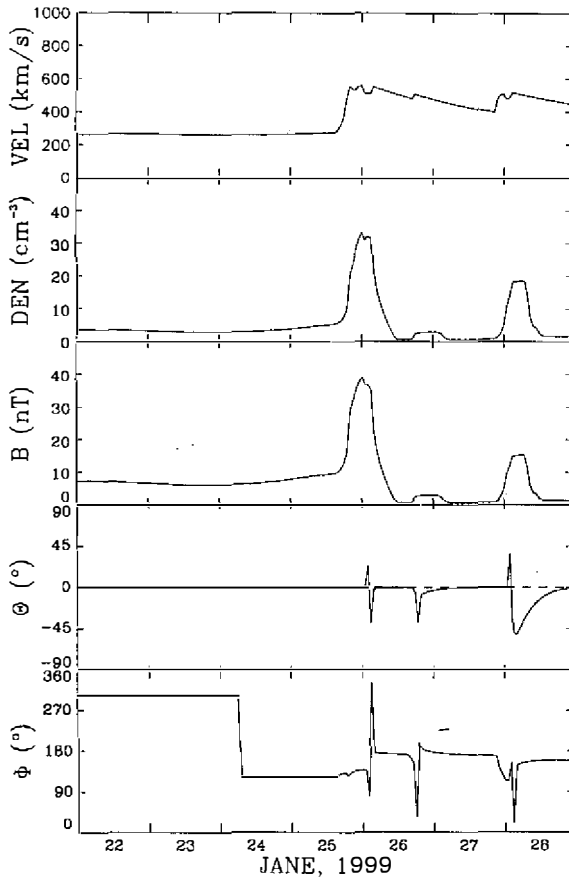


Fig. 5. The calculated variations of the solar wind velocity, the number density, and the IMF B's magnitude, latitude and longitude angles predicted at the Earth's location. Three disturbances and one sector boundary can be seen in these plots.

as can be noticed from the Θ changes. The Φ decreases first and then increases to 180° . IMF B is outward through out the disturbed period.

Now, it is interesting to compare our simulations with the WIND and Geotail observations. Figure 6 shows the parameters of the solar wind and IMF B observed by WIND, which is about 220 Re upstream of the Earth. Interplanetary disturbance from 0200 UT, June 26 to 0700 UT, June 28 can be easily recognized from the magnitude of the IMF B measurements. Higher resolution magnetic field and plasma data show that there are probably three interplanetary transient shocks within this event with one at the front edge, the second at the middle around 2000 UT on June 26 and the third at the back part near ~ 2300 UT, on June 27. Comparison of our simulation with this observations shows that we predict the arrival times of three disturbances reasonable well. The predicted total interval of the event also agrees with observations. However, the simulation fails to predict the angle Φ changes at the front part of the disturbance. WIND observed the inward IMF B for about five hours from about 0300 to 0600 UT on June 26, which is not predicted by the simulation. The B_z prediction does not work because fluctuations of B_z , presumably Alfvén waves, immediately before the arrival of the disturbance present, which is contrary to the assumption of our model that magnetic fields are all in the equatorial plane. The rest of the Φ changes between June 25 and June 29 indicate

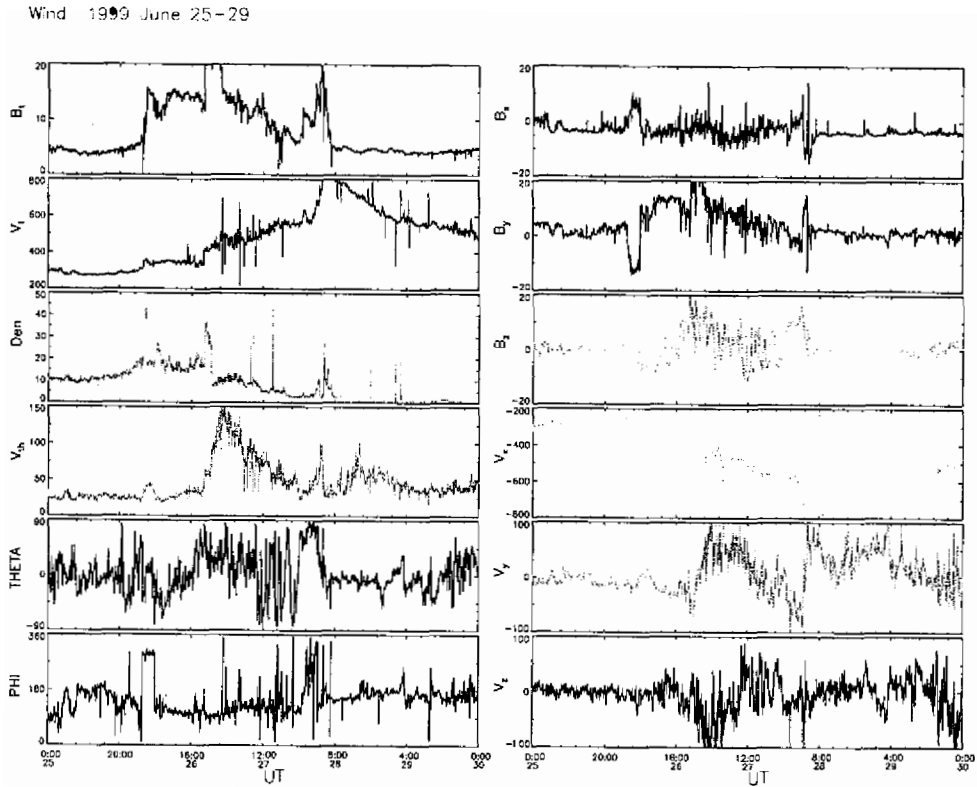


Fig. 6. The solar wind plasmas and magnetic fields for the period June 25-29, 1999 observed by WIND which is located at ~ 220 Re upstream of the Earth's magnetosphere. From the top on the left side are the magnitude of IMF B, solar wind velocity, the number density, the thermal speed of protons, and the IMF's latitude and longitude angles. On the right hand side from the top are the three components of IMF and solar wind velocity respectively.

that our simulation predicts the correct sector.

(3) Earth's bow shock and magnetopause

The disturbance in Fig. 6 lasts for two and half days. The parameters that control the size and shape of the BS and MP are D_p , B_z , β and M_{ms} . Before and after the disturbance, the solar wind plasmas and fields display much less fluctuation. Therefore, when the disturbance interacts with BS and MP, the positions of both BS and MP will change. The changes in position and shape of the BS are given in terms of two parameters γ_0 and α where both are functions of the above four parameters. The γ_0 and α determine the radial distance γ of the BS by the following expression:

$$\gamma = \gamma_0 (1 + \eta) / (1 + \eta \cos \theta)^\alpha,$$

where (γ, θ) are the polar coordinates of the BS surface. The function form of γ_0 and α is

given by Chao et al. (2000) where $\eta = 1.03$. These results can be used to predict the bow shock crossings for the Geotail, which is traveling in a region close to the BS and MP during this time. At this time, the ISTP satellites WIND and ACE are at the Lagrangian points upstream of the Earth. They should observe the solar wind disturbances 30-60 minutes before the Geotail. Figure 7 shows the comparison of the observed B and number density Np by WIND. Since WIND and ACE are always in IP space during this period and Geotail makes BS crossings so that its B changes between the IP and magnetosheath values. Thus, the times that Geotail makes BS crossings are well determined at 1015 UT. The prediction of the BS positions using ACE observations and Geotail's trajectory are shown in Fig. 8. At a given time t, the radial distance γ of the BS is determined from γ_0 , α and θ which are functions of the solar wind parameters and the positions of Geotail. The model predicts that Geotail should cross BS at 1015, 1300 and 1400 UT, respectively. The predictions of 1300 and 1400 UT are not observed.

A magnetopause model (Chao et al., 2000) which has been tested to be quite successful for the predictions of the geosynchronous orbit satellite crossings (Yang et al., 2000) will be used to predict the Geotail's MP crossings caused by this disturbance where the upstream values observed by WIND are used. Now, the functional form for MP is similar to that of BS but γ_0 and α are functions of Dp and Bz only with $\eta = 1.0$. The predicted MP crossings are shown in the lower curve of Fig. 8 at 0100 and 0200 UT on June 29. Geotail also observed these two crossings as can be found in Fig. 7.

(4) Possible ionospheric and ground responses

This disturbance may cause the electrodynamic changes in the equatorial ionosphere. The instrument IPEI on board ROCSAT-1 observed ionospheric bubbles during this period. A sudden increase in AE value at 0515 UT on June 28 is shown in Fig. 9 indicating the onset of a geomagnetic substorm. The other geomagnetic responses are found at Luning station (Yumoto, 1995). The magnitude of B reaches a peak value at 0514 UT as shown in Fig. 10. The power spectra for the time interval from 0510 to 0525 UT is shown in Fig. 11 indicating the presence of some low frequency wave activities. The polar ionosphere is strongly perturbed as the AE suddenly increases. The magnitude and the distribution of field-aligned currents are calculated by the IZMEN model (Papitashvili et al., 1999) and calibrated by the ion drift observations from DMSP satellites shown in Figs. 12(a) and 12(b) for the quiet and perturbed periods, respectively. The currents of both hemispheres in perturbed time increase to about twice that of the quiet time value. In the low latitude ionosphere, the ion density measured by IPEI is shown in Fig. 13 where each horizontal plot represents the measurement for one single orbit of ROCSAT-1. The horizontal axis shows the time for one orbit period of 97 minutes. The next curve from the bottom starts from the end of the previous one. Therefore, the vertical axis gives the numbers for the periods starting from the first one, which is in discrete numbers. These numbers can be converted to time such that the total time spans for the vertical axis is about two and half days. The density depletion regions in the plots show the presence of "bubbles" (Yeh et al., 1999). It is also interesting to note that the low latitude ionosphere shows less diurnal variation in number density of charged particles when the "bubbles" are present (please see Fig. 13). This may be caused by the compression of the magnetosphere during these periods, which might be related to the compression by the inter-

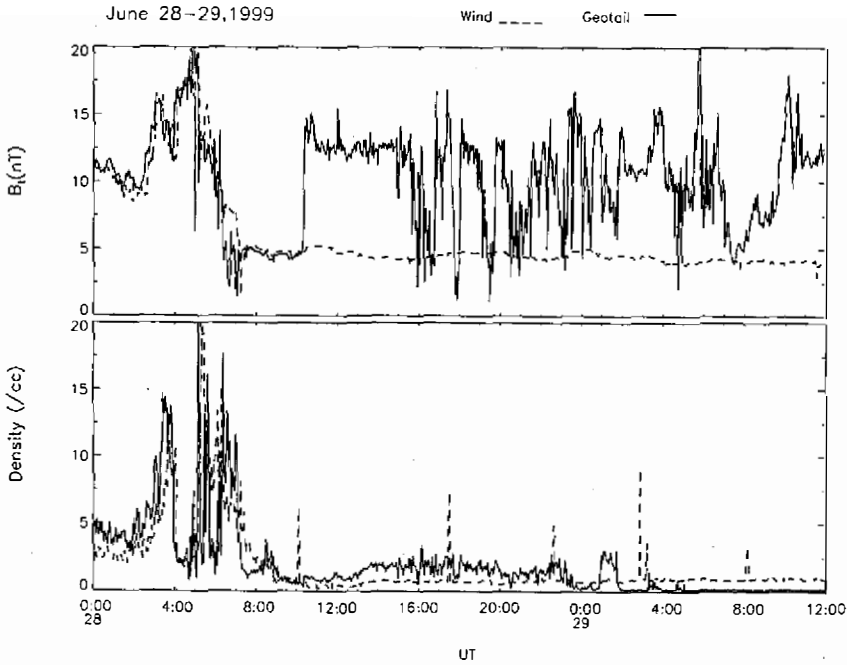


Fig. 7. Comparing the magnitude of magnetic field, B_t and the number density observed by WIND with the same quantities by Geotail. Geotail enters the magnetosheath at ~1000 UT, June 28 and the magnetosphere at 2200 UT June 28 and returns to the magnetosheath at 0100 UT, June 29. Geotail enters the magnetosheath again at 0200 UT, June 29.

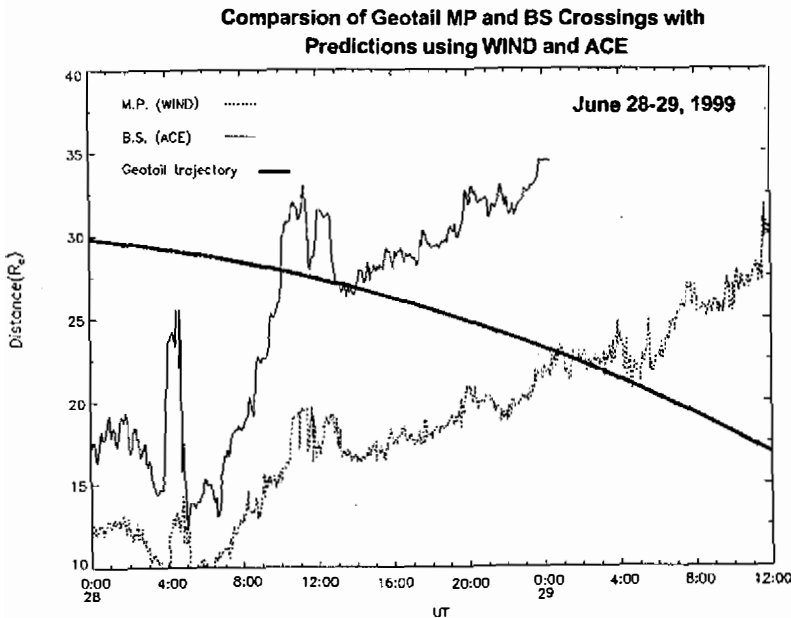


Fig. 8. The predicted bow shock and magneto-pause distances γ during the period June 28-29, 1999. The distance of Geotail from the Earth in R_e is also given by the smooth solid curve.

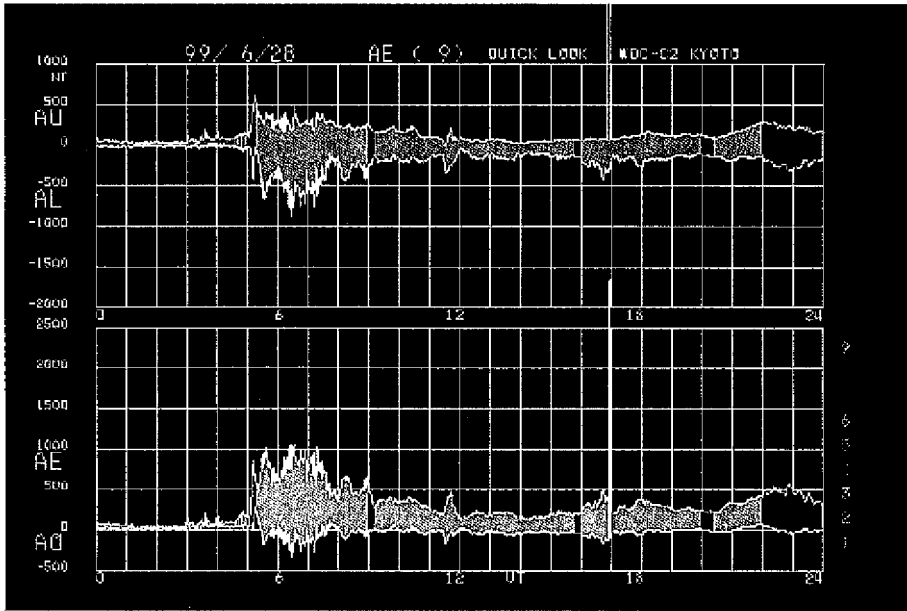


Fig. 9. Geomagnetic index AE, for June 28 1999 shows geomagnetic substorm activities during this period.

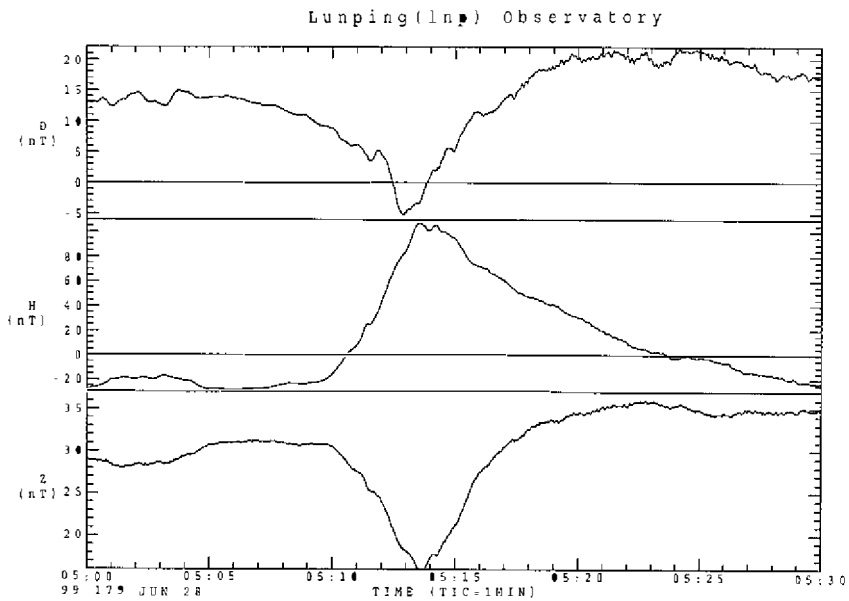


Fig. 10. Flux gate magnetometer data measured at Luning station for June 28, 1999. The south-north H, the east-west D and vertical Z components are shown.

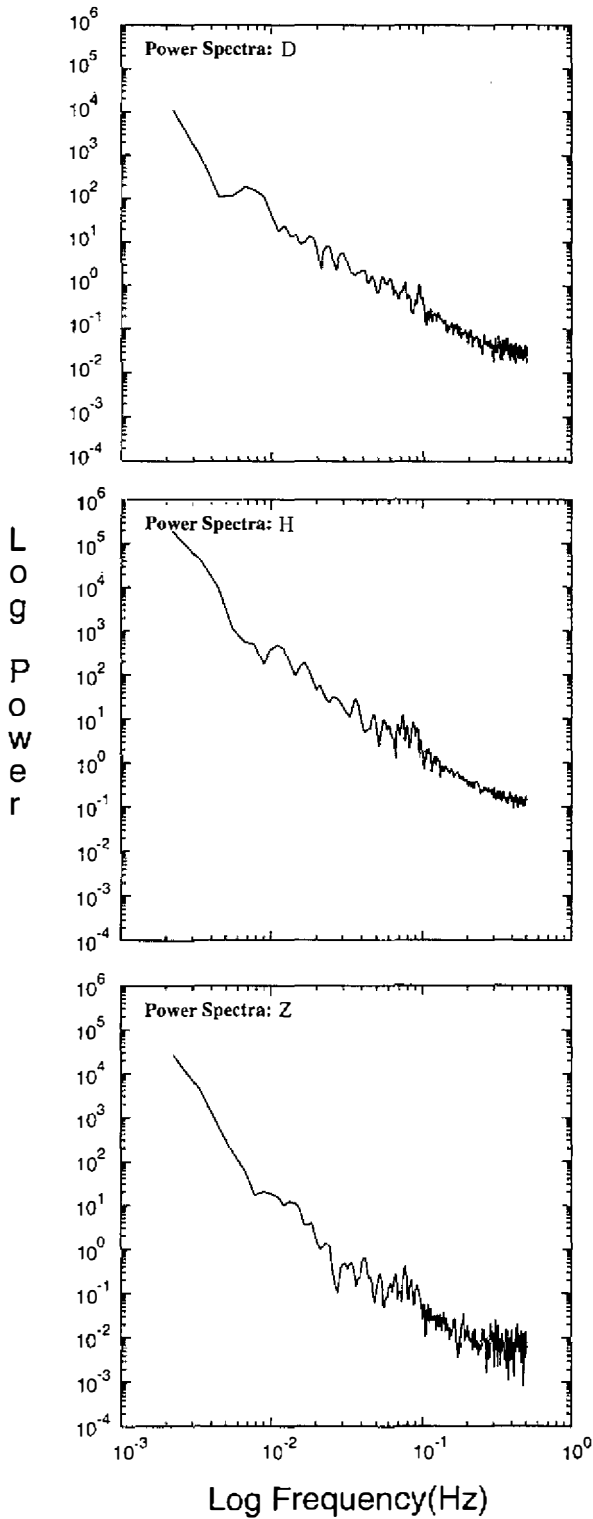


Fig. 11. Power spectrum for the period from 0510 to 0525 UT for each of the components shown in Fig. 10. Geomagnetic micropulsation of type Pc-4 is present.

IZMEM Calibrated by DMSP Ion Drift Observations

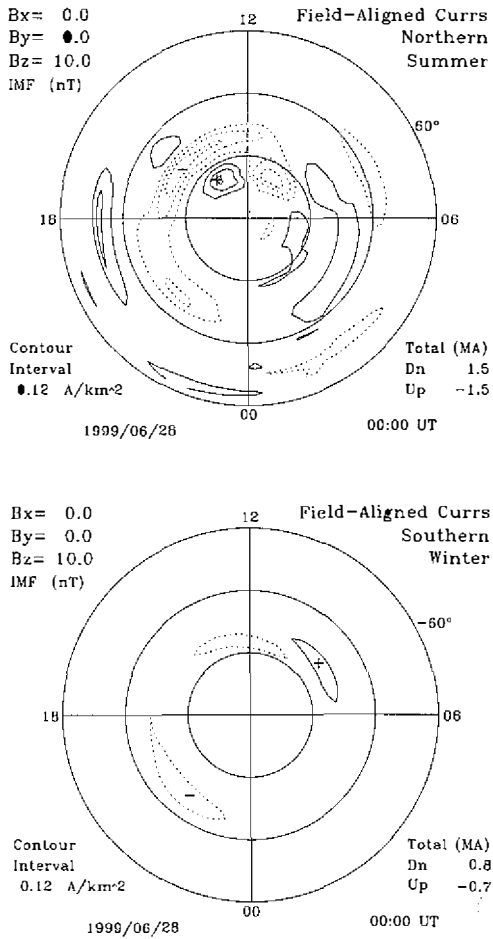


Fig. 12(a). Using IZMEM model calibrated by DMSP ion drift observations to generate the field-aligned currents for the quiet period. The top one is for the northern polar hemisphere and the bottom one is for southern polar hemisphere.

planetary disturbances and the increases in ionized oxygen in the night side region.

5. DISCUSSION AND SUMMARY

Research in solar-terrestrial physics has been conducted for many years. Only in the last few years have serious efforts been given to applying the findings for space weather prediction. Since we still have many problems in each of the areas: the Sun, the interplanetary space and the magnetosphere as well as their couplings, the predictions we have attempted are very preliminary. Nevertheless, the scheme we outline above can offer useful results for space weather study.

On the solar side, the causes for adverse space weather need to be identified. Through many years of study, the space physics community generally considers CMEs the most important cause, as compared to other solar activities, such as flares, filament eruptions, and coronal

IZMEM Calibrated by DMSP Ion Drift Observations

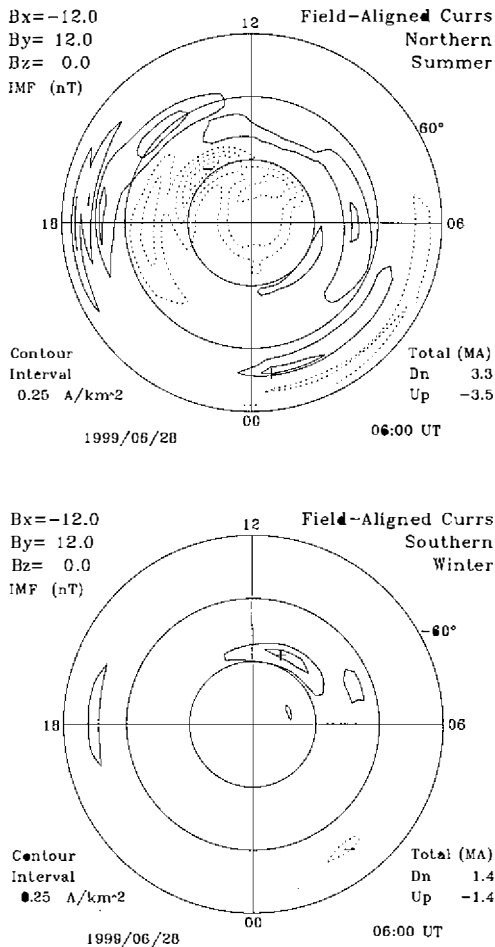


Fig. 12(b). Same plots as in Fig. 12(a) for the disturbed periods of June 28, 1999. The only input from interplanetary space is the IMF B_x and B_y . Note the enhancement of field-aligned currents during this period.

holes. These solar activities and the CME might be interrelated and the physics of their relationship is still not very clear. Therefore, for practical purposes, we take CMEs as the basis for the space weather prediction.

The ability to predict a CME release from the solar corona is still a long way off. The direct way to find the source is to observe the eruption of CMEs. The early satellites, like Skylab, SMM, and the recent SOHO can measure the CMEs seen only at the limb. The CMEs propagating earthward are observed as halo CMEs by SOHO. It is difficult to observe the head-on type CMEs. Hence, we take the next most likely source, a filament eruption as our disturbance. Once the source is selected, we have to describe how such a disturbance propagates from the solar corona to the vicinity of the Earth.

Numerical simulations have been the most common practice for the propagation of solar-interplanetary disturbances. Because of the non-uniform nature of the solar corona and interplanetary space, it is not easy to simulate such phenomena in 3-dimensional space with all the

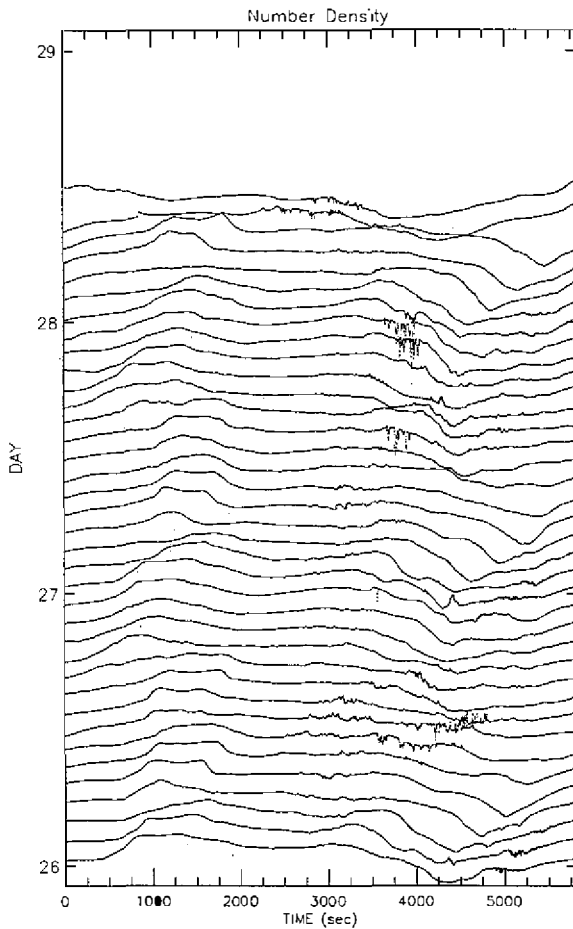


Fig. 13. Ion number density measured by IPEI of ROCSAT-1 for the period from June 26 to June 28, 1999. The density shows cavities indicating “bubbles” in the equatorial ionosphere which may relate to the interplanetary disturbance. The horizontal length is one orbital period for ROCAST-1, which equals to 97 minutes.

inhomogeneities included. It is generally believed that the MHD simulations can give a fairly good description of the propagation and interactions of all the three MHD wave modes. One would expect that the various types of discontinuities such as the fast, slow, intermediate shocks, rotational and tangential discontinuities, could be generated in such simulations. Without including the effect of the rotation of the Sun and the general non-uniform coronal background, Wu et al. (1999) simulate the famous January sun-earth connection event. A large amount of super-computer time is needed for just one such single simulation. On the other hand, we use a simple kinematic model, which cannot account for the interactions of the MHD wave modes but can describe the supersonic flows evolving in interplanetary space. The boundaries between the flare (or CMEs) ejecta and the ambient solar wind in general represent the fast shock surfaces. The effects of solar rotation and the non-uniform surface-magnetic field are included in a crude way in this simulation. By incorporating multi-satellite observations, it is possible to derive the shape and size of the interplanetary disturbances. The example of the June 24-28, 1999 event demonstrates the usefulness of this kinematic model. This kind of simulation can be performed even on a personal computer. Because it is ease to use and efficient, we hope to develop its capability for space weather prediction.

The BS and MP are the most important boundaries of the Earth's magnetosphere. They protect us from the direct damage by the solar wind and some energetic particles. The prediction of the positions and shape of the BS and MP is very essential for space weather prediction. But, before a good prediction for the detailed structures of the solar wind made from the solar source is available, predictions of changes of the locations and shape of BS and MP mainly rely on the upstream observations of the magnetosphere. Fortunately, the ISTP satellites, particularly the WIND and ACE are very useful for such purposes. Our models for the BS and MP respectively have demonstrated very accurate predictions for many events and hope they will be implemented for space weather prediction in the near future.

The responses inside the Earth's magnetosphere due to the solar and interplanetary disturbances are under very active study particularly for space weather studies. The energy transfer function \mathcal{E} needs further study so that the magnetosphere response can be more accurately calculated. The field-aligned currents due to interplanetary Alfvén waves and rotational discontinuities need to be incorporated in the ionospheric circulation models such as the AMIE, IZMEN and others. The global distribution of ionospheric electron density and the polar region field-aligned currents obtained from the COSMIC project would provide valuable data for the study of ionospheric response to the adverse space weather.

In summary, we have demonstrated a scheme for modeling solar disturbances, which propagate through the interplanetary space and interact with the Earth's magnetosphere causing changes of the BS, MP and the polar and equatorial ionospheres. Comparison with observations in these regions shows this prediction scheme warrants further development.

Acknowledgments This work is supported by grants from the National Science Council in Taiwan, ROC to National Central University (NSC88-NSPO(B)-RS3-FA07-01) and National Cheng Kung University (NSC 89-2111-M-006-001). J.K.C. would like to thank the ISTP group for the solar wind plasma and magnetic field data. J.K.C. also appreciate the help from Dr. Ching Huei Lin for preparing many figures used in this work. Discussions with all the members in the Data Environment Center, Institute of Space Science, NCU are appreciated.

REFERENCES

- Akasofu, S. -I., and J. K. Chao. 1980: Interplanetary Shock Waves and Magnetospheric Substorms. *Planet. Space Sci.*, **28**, 381-385.
- Akasofu, S. -I., 1981: 'Energy Coupling between the Solar Wind and the Magnetosphere'. *Space Sci. Rev.*, **28**, 111.
- Akasofu, S. I., and C. F. Fry, 1986: A first generation numerical geomagnetic storm prediction scheme. *Planet. Space. Sci.*, **34**, 77-92.
- Baker, D. N., R. L. McPherron, T. E. Cayton, and R. W. Klebesadel, 1990: Linear prediction filter analysis of relativistic electron properties at 6.6 Re. *J. Geophys. Res.*, **95**, 15133-15140.
- Bame, S. J., J. R. Asbridge, W. C. Feldman, E. E. Fenimore, and J. T. Gosling., 1979: Solar wind heavy ions from flare-heated coronal plasma. *Solar Phys.*, **62**, 179.
- Bennett, L, M. G. Kivelson, K. K. Khurana, L. A. Frank and W. R. Paterson, 1997: A model

- of Earth's distant bow shock. *J. Geophys. Res.*, **102**, 26,927-26,941.
- Bravo, S., X. Blanco-Cano, and C. Lopez, 1999: Characteristics of interplanetary magnetic clouds in relation to their solar association. *J. Geophys. Res.*, **104**, 581-591.
- Burlaga, L. F., Behannon, K. W., and Klein, L. W.: 1987, 'Compound Streams, Magnetic Clouds and Major Geomagnetic Storms'. *J. Geophys. Res.*, **92**, 5725-5734.
- Burton, R. K., R. I. McPherron, and C.T. Russell, 1975, An empirical relationship between interplanetary conditions and Dst. *J. Geophys. Res.*, **80**, 4204-4229.
- Chao, J. K., 1973: Steepening of Nonlinear Waves in the Solar Wind. *J. Geophys. Res.*, **78**, 5411-5424.
- Chao, J. K., 1974: A Model for the Propagation of Flare-Associated Interplanetary Shock Waves, in Solar Wind 3. In: C. T. Russell (Ed.), UCLA, 169.
- Chao, J. K. and R. P. Lepping, 1974: A Correlative Study of SSC's Interplanetary Shocka, and Solar Activity, Presented to the Conference of Flare-Produced Shock Waves in the Corona and Interplanetary Space, Boulder, Colorado, Sept. 11-14,1972. *J. Geophys. Res.* **79**,1799.
- Chao, J. K. et al., 1999: A model for the size and shape of the Earth's bow shock, AGU 1999 FALL MEETING, (SM51A-04) F897.
- Cairns, I. H., D. H. Fairfield, R. R. Anderson, V. H. Carlton, K. I. Paularena, and A. J. Lazarus, 1995: Unusual locations of Earth's bow shock on September 24-25, 1987: Mach number effects. *J. Geophys. Res.*, **100**, 47-62.
- Cairns, I. H., and J. G. Lyon, 1995: MHD simulations of Earth's bow shock at low Mach number: Standoff distances. *J. Geophys. Res.*, **100**, 17173-17180.
- Chen, J., Peter J. Cargill, and Peter J. Palmadesso, 1997: Predicting solar wind structures and their geoeffectiveness. *J. Geophys. Res.*, **102**, 14,701-14,720.
- Dryer, M., 1982: Coronal transient phenomena. *Space Sci. Rev.*, **33**, 233.
- Dryer, M., 1994: Interplanetary studies: propagation of disturbances between the Sun and the magnetosphere. *Space Sci. Rev.* **67(3/4)**, 363-419.
- Fairfield, D. H., 1971: Average and unusual locations of the Earth's magnetopause and bow shock. *J. Geophys. Res.*, **76**, 6700-6716.
- Farris, M. H., and C.T. Russell, 1994: Determining the standoff distance of the bow shock: Mach number dependence and use of models. *J. Geophys. Res.*, **99**, 17681-17689.
- Formisano, V., V. Domingo, and K.-P. Wenzel, 1979: The three-dimension shape of the magnetopause. *Planet. Space Sci.*, **27**, 1137.
- Gonzalez, W. D., and B. T. Tsurutani, 1987: Criteria of interplanetary parameters causing intense geomagnetic storms (Dst < -100nT). *Planet. Space Sci.*, **35**, 1101-1109.
- Gosling, J. T., 1975: Large-scale inhomogeneities in the solar wind of solar origin. *Rev. Geophys.*, **13**, 1053.
- Gosling, J. T., J. McComas, J. L. Phillips, and S. J. Bame, 1991: Geomagnetic activity associated with Earth passage of interplanetary shock disturbances and coronal mass ejections. *J. Geophys. Res.*, **96**, 7831-7839.
- Gosling, J. T., 1993: The solar flare myth. *J. Geophys. Res.*, **98**, 18,937-18,949.
- Hakamada, K., and S. I. Akasafu, 1982: Simulation of three- dimensional solar wind distur-

- bances and resulting geomagnetic storms. *Space Science Rev.*, **31**, 3-70.
- Harrison, R. A., 1994: A statistical study of the coronal mass ejection phenomena. *Adv. Space Res.*, **14**(4), 23-28.
- Hirshberg, J., A. Alksne, D. S. Colburn, S. J. Bame, and A. J. Hundhausen, 1970: Observation of a solar flare induced interplanetary shock and helium-enriched driver gas. *J. Geophys. Res.*, **75**, 1-15.
- Hoeksema, J. T., and X. Zhao, 1992: Prediction of magnetic orientation in driver gas associated -Bz events. *J. Geophys. Res.*, **97**, 3151-3156.
- Hundhausen, A. J., 1972: Coronal expansion and solar wind, Springer, Berlin Heidelberg, New York.
- Hundhausen, A. J., 1993: Sizes and locations of coronal mass ejections: 1993, SMM observations from 1980 and 1984-1989. *J. Geophys. Res.*, **98**, 13,177-13200.
- Joselyn, J. A., and P. S. McIntosh, 1981: Disappearing solar filaments: A useful predictor of geomagnetic activity. *J. Geophys. Res.*, **86**, 4555-4564.
- Joselyn, J. A., 1995: Geomagnetic activity forecasting: The state of the art. *Rev. Geophys.*, **33**, 383.
- Kan, J. R., and L. C. Lee, 1979: Energy coupling function and solar wind-magnetosphere dynamo. *Geophys. Res. Lett.*, **6**, 577-580.
- Klein, L. W., and L. F. Burlaga, 1982: 'Interplanetary Magnetic Clouds at 1 AU'. *J. Geophys. Res.*, **87**, 613-624.
- Ma, Z. W., and L. C. Lee, 1999: A simulation study of generation of field-aligned currents and Alfvén Waves by three-dimensional magnetic reconnection. *J. Geophys. Res.*, **104**, 10,177-10,189.
- McComas, D. J., J. T. Gosling, S. J. Bame, E. J. Smith, and H. V. Cane, 1989: A test of magnetic field draping induced Bz perturbations ahead of fast coronal mass ejections. *J. Geophys. Res.*, **94**, 1465-1471.
- Odstrčil, D., and V. J. Pizzo, 1999: Three-dimensional propagation of coronal mass ejections (CMEs) in a structured solar wind flow 1, CME launched within the streamer belt. *J. Geophys. Res.*, **104**, 483-492.
- Papitashvili, V. O., F. J. Rich, M. A. Heinemann, and M. R. Hairston, 1999, Parameterization of the Defense Meteorological Satellite Program ionospheric electrostatic potentials by the interplanetary magnetic field strength and direction. *J. Geophys. Res.*, **104**, 177-184.
- Peredo, M., J. A. Slavin, E. Mazyr, and S. A. Curtis, 1995: Three-dimensional position and shape of the bow shock and their variation with Alfvénic, sonic and magnetosonic Mach numbers and interplanetary magnetic field orientation. *J. Geophys. Res.*, **100**, 7907-7916.
- Perreault, P., and S.-I. Akasofu, 1978: A study of geomagnetic storms. *Geophys. J. R. Astron. Soc.*, **54**, 547.
- Petrinec, S. M., and C. T. Russell, 1993: An empirical model of the size and shape of the near-Earth magnetotail. *Geophys. Res. Lett.*, **20**, 2695.
- Petrinec, S. M., and C. T. Russell, 1996: Near-Earth magnetotail shape and size as determined from the magnetopause flaring angle. *J. Geophys. Res.*, **101**, 137-152.

- Richmond, A. D. and Y. Kamide, 1988: Mapping electrodynamic features of the high-latitude ionosphere from localized observations: technique. *J. Geophys. Res.*, **93**, 5741-5759.
- Richmond, A. D., 1992: Assimilative mapping of ionospheric electrodynamics. *Adv. Space Res.*, **12**, (6)59-(6)68.
- Richmond, A. D., G. Lu, B. A. Emery, and D. J. Knipp, 1998: The AMIE procedure: Prospects for space weather specification and prediction. *J. Geophys. Res.*, 103-112.
- Roelof, E. C., and D. G. Sibeck, 1993: Magnetopause shape as a bivariate function of interplanetary magnetic field Bz and solar wind dynamic pressure. *J. Geophys. Res.*, **98**, 21,421-21,450.
- Russell, C. T., and R. J. McPherron, 1973: Semiannual variation of geomagnetic activity. *J. Geophys. Res.*, **78**, 92-95.
- Sharma, A. A., D. V. Vassiliadis, and K. Papadopoulos, 1993: Reconstruction of low-dimensional magnetospheric dynamics by singular spectrum analysis. *Geophys. Res. Lett.*, **20**, 335-338.
- Sheeley, N. R. Jr., R. A. Howard, M. J. Koomen, D. J. Michels, R. Schwenn, K. H. Muhlhauser and H. Rosenbaure, 1985: Coronal mass ejections and interplanetary shocks. *J. Geophys. Res.*, **90**, 163-175.
- Shue, J. H., J. K. Chao, H. C. Fu, C. T. Russell, P. Song, K. K. Khurana, and H. J. Singer, 1997: A new functional form to study the solar wind control of magnetopause size and shape. *J. Geophys. Res.*, **102**, 9497-9511.
- Shue, J. H., P. Song, C. T. Russell, J. T. Steinberg, J. K. Chao, G. Zastenker, O. L. Vaisberg, S. Kokubun, H. J. Singer, T. R. Detman, and H. Kawano, 1998: Magnetopause location under extreme solar wind conditions. *J. Geophys. Res.*, **103**, 17,691-17,700.
- Shue, J. H., P. Song, C. T. Russell, J. K. Chao, Y. H. Yang, H. J. Singer, 2000: Toward forecasting geosynchronous magnetopause crossings for space weather. *J. Geophys. Res.*, (in press).
- Slavin, J. A., and R. E. Holzer, 1981: Solar wind flow about the terrestrial planets, 1, 1981, Modeling bow shock position and shape. *J. Geophys. Res.*, **86**, 11401-11418.
- Sun, W., and S. I. Akasofu, 1985: Calibration of the Kinematic Method of Studying Solar Wind Disturbances on the Basis of a One-dimensional MHD Solution and a Simulation Study of the Heliospheric Disturbances between 22 November and 6 December 1977. *Planet. Space Sci.*, **33**, 933-943.
- Tang, F., B. T. Tsurutani, W. D. Gonzalez, S. I. Akasofu, and E. Smith, 1989: Solar sources of interplanetary southward Bz events responsible for major magnetic storms (1978-1979). *J. Geophys. Res.*, **94**, 3535-3541.
- Tsurutani, B. T., C. T. Russell, J. H. King, R. J. Zwickl, and R. P. Lin, 1984: "A Kinky Heliospheric Current Sheath: Causes of the CDAW6 Substorms". *Geophys. Res. Lett.* **11**, 339.
- Tsurutani, B. T., W. D. Gonzalez, F. Tang, S. I. Akasofu, and E. Smith, 1988: Origin of interplanetary southward magnetic fields responsible for major magnetic storms near solar maximum (1978-1979), *J. Geophys. Res.*, **93**, 8519-8531.
- Tsurutani, B. T., Ho, C. M., Arballo, J. K., Goldstein, B. E. and Balogh, A.: 1995: "Large Amplitude IMF Fluctuations in Corotating Interaction Regions: Ulysses at

- Midlatitudes". *Geophys. Res. Lett.* **22**, 3397.
- Tsurutani, B. T., and W. D. Gonzalez, 1997: "The interplanetary Causes of Magnetic Storms: A Review". In: B. T. Tsurutani, W. D. Gonzalez and Y. Kamide (Eds.), *Magnetic Storms*, Amer. Geophys. Union Press, Washington D.C.. Mon. Ser. 98, p.77-89.
- Tsurutani, B. T., Y. Kamide, W. D. Gonzalez, and R. P. Lepping, 1999: "Interplanetary Causes of Great and Superintense Magnetic Storms", *Physics and Chemistry of the Earth*, in press.
- Vassiliadis, D., A. J. Klimas, D. N. Baker, and D. A. Roberts, 1995: A description of solar wind-magnetosphere coupling based on nonlinear filters. *J. Geophys. Res.*, **100**, 3495-3512.
- Webb, D. F., and A. J. Hundhausen, 1987: Activity associated with the solar origin of coronal mass ejections. *Solar Phys.*, **108**, 383-390.
- Wilson, R. M., and E. Hildner, 1984: Are interplanetary magnetic clouds manifestations of coronal transients at 1 AU?. *Sol. Phys.*, **91**, 169.
- Wilson, R. M. and E. Hildner, 1986: On the association of magnetic clouds with disappearing filaments. *J. Geophys. Res.*, **91**, 5867-5872.
- Wright, C. S., and L. F. McNamara, 1983: The relation between disappearing solar filaments, coronal mass ejections and geomagnetic activity. *Solar Phys.*, **87**, 401-417.
- Wu, Chin-Chun, and M. Dryer, 1996: Predicting the initial IMF Bz polarity's Change at 1 AU caused by shocks that precede coronal mass ejections, *Geophys. Res. Lett.*, **23**, 1709-1712.
- Wu, J.-G., and H. Lundstedt, 1996, Prediction of geomagnetics storms from solar wind data using Elman recurrent neural network. *Geophys. Res. Lett.*, **23**, 319-322.
- Wu, D. J., J. K. Chao, and R. P. Lepping, 2000: Interaction between an interplanetary magnetic cloud and the Earth's magnetosphere: Motion of the bow shock. *J. Geophys. Res.*, (in press).
- Wu, S. T., W. P. Guo, D. J. Michels, and L. F. Burlaga, 1999: MHD description of the dynamical relationships between a flux-rope, streamer, coronal mass ejection (CME) and magnetic cloud: an analysis of the 1997 January sun-earth connection event. *J. Geophys. Res.* **104(7)**, 14789-14801.
- Yang, et. al., 1999: prediction of the magnetopause location under extreme solar wind conditions, (SM51A-07) AGU 1999 FALL MEETING, F898.
- Yeh, H. C., S. I. Su, R. A. Heelis, J. M. Wu, ROCSAT-1, 1999: IPEI Preliminary Result: Vertical Ion Drift Statistics. *TAO*, **10**, 805-820.
- Yumoto, K., and the 210° MM Magnetic Observation Group, 1995: The 210° MM Magnetometer network, IUGG XXI General Assembly, held at Boulder, Colorado, July 2-14.
- Zhao, X., and J. Todd Hoeksema, 1995: Prediction of the interplanetary magnetic field strength. *J. Geophys. Res.*, **100**, 19-33.
- Zwan, B. J., and R. A. Wolf, 1976: "Depletion of the Solar Wind Plasma Near a Planetary Boundary". *J. Geophys. Res.*, **81**, 1636-1648.